Two Apolipoprotein E Mimetic Peptides, ApoE(130−149) and ApoE(141−155)^2, Bind to LRP1[†]

Johnny E. Croy, Theodore Brandon, and Elizabeth A. Komives*

Department of Chemistry and Biochemistry, University of California at San Diego, 9500 Gilman Drive, La Jolla, California 92093-0378

Received December 8, 2003; Revised Manuscript Received April 5, 2004

ABSTRACT: LRP1 is a cell surface receptor responsible for clearing some 30 known ligands. We have previously shown that each of the three complete LDL receptor-homology domains of the LRP1 extracellular domain (sLRPs) binds apoE-enriched β-VLDL particles. Here we show that two peptides from the N-terminal receptor binding domain of apoE, which are known to elicit a number of different cellular responses, bind to LRP1. Solution binding assays show that the two peptides, apoE(130−149) and apoE-(141−155)^2, interact with each of the sLRPs (2, 3, and 4). Each peptide was found to exhibit the same solution binding characteristics as apoE-enriched β-VLDL particles. Surface plasmon resonance analyses of the sLRP−apoE peptide interaction show that both peptides bind the sLRPs with K_D values in the 100 nM range, a value similar to the effective concentration required for observation of the cellular responses. Consistent with results from mutagenesis studies of binding of apoE to LDLR, apoE(130−149,Arg142Glu) bound with a K_D similar to that of the wild-type sequence, while apoE(130−149,Lys143Glu) showed a 10-fold decrease in K_D. Each of the peptides bound heparin, and heparin competed for sLRP binding.

Apolipoprotein E (apoE)[1] is an important protein involved in the metabolism and transportation of lipids and cholesterol in humans (for a review, see ref *1*). Cellular uptake of apoE involves internalization by members of the LDL receptor superfamily, including the low-density lipoprotein (LDL) receptor and LDL receptor-related protein 1 (LRP1). In addition to its transport function, apoE has been implicated in neuronal growth and repair (*2*, *3*) and consequently has been found to be involved with the progression of late onset familial Alzheimer's disease (*4*−*6*).

ApoE is a 34 kDa two-domain protein (*7*, *8*). The 22 kDa, N-terminal domain has been shown to be responsible for receptor binding, and the crystal structure of this fragment shows that the domain folds into an elongated, four-helix bundle (*9*). A cluster of positively charged residues (residues 139−169) found in helix 4 has been suggested to be important for receptor interaction (*9*−*11*) and heparin binding (*12*, *13*). Additionally, three dominant isoforms have been observed in humans, and these sequence variations occur in the N-terminal domain: **E2** (Cys^{112} and Cys^{158}), **E3** (Cys^{112} and Arg^{158}), and **E4** (Arg^{112} and Arg^{158}) (*14*). ApoE2 was shown to be defective in LDL receptor binding, leading to increases in plasma lipid levels and familial hypercholestemia (*15*). Patients homozygous for apoE4 have a higher incidence of Alzheimer's disease (*6*). ApoE3 seems to provide protection from the harmful effects of the other two isoforms. Single-point mutations within the N-terminal domain (Lys143Ala and Leu144Pro) cause an approximate 90% loss in the ability to compete for [^{125}I]LDL binding to fibroblasts (*16*), suggesting that these residues are essential to receptor binding interactions.

In addition to lipid transport, studies have shown that apoE causes a number of different cellular responses. The N-terminal domain of apoE has been shown to be neurotoxic when applied to primary neurons in culture (*17*). Synthetic peptides from the N-terminal domain also elicit a number of different cellular responses (*18*−*20*). Clay *et al.* (*21*) showed that a monomeric stretch of residues 130−149 and a synthetic tandem repeat of residues 141−155, termed apoE-(141−155)^2, caused cytostatic and cytotoxic effects on IL2-dependent T lymphocytes, similar to the effects observed with the full-length N-terminal domain. Moulder *et al.* (*18*) showed that apoE(141−155)^2 was neurotoxic to superior cervical ganglion cells. Laskowitz *et al.* (*20*) showed that apoE(130−149) and apoE(141−155)^2 downregulate microgilal activation, and Misra *et al.* (*19*) showed that these peptides initiate a calcium-dependent signaling response in macrophages. The mechanism by which these cellular responses are elicited has remained elusive, although several groups have speculated that the observed effects might be mediated by LRP1 (*19*, *21*, *22*). Others have refuted the idea of the participation of LRP1 in these processes on the basis of the observation that RAP does not alleviate the bioactivity of these peptides (*18*, *20*).

The studies presented here investigate the binding of the bioactive apoE peptides, apoE(130−149) and apoE(141−155)^2, to each LDL receptor-homology region of LRP1 (sLRP2, -3, and -4). Solution binding experiments show that the apoE peptides bind to each sLRP fragment of LRP1 with similar high affinity. As was also observed for full-length

[†] This work was supported by NIH Grant AG17992.

* To whom correspondence should be addressed. Phone: (858) 534-3058. Fax: (858) 534-6174. E-mail: ekomives@ucsd.edu.

[1] Abbreviations: LDL, low-density lipoprotein; LRP1, low-density lipoprotein receptor-related protein 1; apoE, apolipoprotein E; VLDL, very low-density lipoprotein; RAP, receptor-associated protein; EDTA, ethylenediaminetetraacetate; MALDI-TOF, matrix-assisted laser desorption ionization time-of-flight; GlcNAC, *N*-acetylglucosamine; CD, circular dichroism; SPR, surface plasmon resonance; SA, streptavidin.

10.1021/bi036208p CCC: $27.50
Published on Web 05/20/2004

Table 1: Characterization of Synthetic ApoE Peptides

peptide	sequence	theoretical MW[a]	MALDI MW	size exclusion
apoE(141−155)^2	LRKLRKRLLRDADDLLRKLRKRLLRDADDL	4194.3	4194	dimer
apoE(130−149)	TEELRVRLASHLRKLRKRLL	2938.5	2939	monomer
apoE(130−149,Arg142Glu)	TEELRVRLASHLEKLRKRLL	2911.5	2911	ND
apoE(130−149,Lys143Glu)	TEELRVRLASHLRELRKRLL	2939.5	2939	ND
apoE(130−149,scrambled)	LREKKLRVSALRTHRLELRL	2938.5	2939	ND

[a] The molecular weights include the linked biotin group that was added to the N-terminus of each peptide.

apoE-enriched β-VLDL particles, binding was not challenged by GST−RAP or by treatment with EDTA, but was challenged by lactoferrin (*23*). The kinetic parameters that govern the binding of each bioactive apoE peptide binding to each sLRP, as well as the binding of two point mutant peptides to sLRP2, were measured using surface plasmon resonance. The ability of each bioactive apoE peptide to bind heparin was also assessed, and heparin was shown to compete for binding of sLRP to each bioactive apoE peptide.

MATERIALS AND METHODS

Chemicals, Reagents, and Proteins. All chemicals unless otherwise noted were purchased from Fisher Scientific and were of the highest available purity. N^{α}-Fmoc amino acids with benzyl-based side chain protecting groups and PEG-PAL-PS resin were purchased from Applied Biosystems. The glutathione *S*-transferase fusion protein with human RAP (GST−RAP) was prepared as described previously (*24*). Apolipoprotein E-enriched β-VLDL was purchased from Intracel, Inc.

Synthesis of ApoE(130−149) and ApoE(141−155)^2. Peptides were synthesized with N-terminal biotinylation and C-terminal amides on an Applied Biosystems 9050 peptide synthesizer. The naturally occurring sequence from the N-terminal domain of apoE, residues 130−149, was prepared as biotin-TEELRVRLASHLRKLRKRLL-amide and is termed apoE(130−149). The synthetic tandem repeat of residues 141−155 was prepared as biotin-LRKLRKRLLRDADDLL-RKLRKRLLRDADDL-amide and is termed apoE(141−155)^2. A scrambled control peptide and two point mutant peptides of apoE(130−149) were also synthesized (Table 1). All of the peptides were specifically biotinylated with a 1.3-fold molar excess of EZ-Link Sulfo-NHS-LC-LC-Biotin (Pierce Chemicals) on the N-terminus prior to deprotection. Each peptide was purified by reverse phase HPLC on a Waters C18 column (300 mm × 19 mm) using a 60 min linear gradient of 0.1% trifluoroacetic acid to 50% acetonitrile. Each apoE peptide eluted between 38 and 42% acetonitrile. The peptide identity and purity were determined by MALDI-TOF mass spectrometry, and purified apoE peptides were stored at 10 mg/mL in H_2O at pH 7.0 and −70 °C.

Solution Binding Studies of Each sLRP with Apolipoprotein E-Enriched β-VLDL. Each of the three complete LDL-like domains of LRP1 (sLRP2, sLRP3, and sLRP4) was expressed with a C-terminal FLAG epitope and purified as previously described (*23*). The proteins were shown to be monomeric after deglycosylation with Endo H, which leaves the core GlcNAC at each N-linked glycosylation site. Capture of apoE-enriched β-VLDL particles was also performed as previously described (*23*). Briefly, apoE-enriched β-VLDL particles (Intracel, Inc.) (7.5 μg) were mixed with 5 μg of each sLRP−FLAG fragment (2, 3, and 4) in a volume of 1 mL at 37 °C for 2 h. Complexes were captured using a monoclonal anti-FLAG antibody (Sigma Chemicals) covalently linked to agarose beads. ApoE−sLRP complexes were separated via reducing 13% SDS−PAGE and transferred to nitrocellulose, and the blots were probed for the presence of apoE with a polyclonal anti-apoE antibody (Chemicon). To test for the calcium dependence of binding, some binding experiments were carried out in 10 mM Hepes (pH 7.4), 150 mM NaCl, and 20 mM EDTA (MB150EDTA). Competition for binding by GST−RAP was assessed by including a 50-fold molar excess of GST−RAP in the binding experiment. Competition for binding by lactoferrin was assessed by including a 3-fold molar excess of lactoferrin in the binding experiment. Competition for binding by apoE-(130−149) was assessed by addition of a 10-fold molar excess of apoE(130−149) in the binding experiment.

Solution Binding Studies of Each sLRP with ApoE(130−149) and ApoE(141−155)^2. Streptavidin (SA)−agarose beads (1 mL slurry) were equilibrated in 20 mM Hepes (pH 7.4), 150 mM NaCl, 2.5 mM $CaCl_2$, and 1 mM $MgCl_2$ (MB150 buffer) for 2 h and then mixed with each biotinylated apoE peptide (500 μg) for 4 h at 25 °C. The beads were washed exhaustively and stored at 4 °C in MB150 buffer with 0.02% azide. Prior to the capture of sLRPs with apoE(141−155)^2, it was necessary to first incubate this peptide in high-salt buffer containing 20 mM Hepes (pH 7.4), 500 mM NaCl, 2.5 mM $CaCl_2$, and 1 mM $MgCl_2$ (MB500 buffer) at 4 °C for 30 min. This treatment apparently structures the peptide in such a way that it becomes binding competent (manuscript in preparation). Capture of the sLRPs with ApoE(130−149) did not require preincubation in MB500 buffer for binding. For each pull-down experiment, sLRPs (10 μg) were mixed with 50 μL (packed volume) of peptide beads at room temperature for 1 h on a rotating platform. Control experiments were carried out either with SA−agarose beads to which no peptide had been bound, or with beads containing the scrambled peptide.

RAP competition was assessed by preincubating a 50-fold molar excess of GST−RAP with each sLRP fragment at 37 °C for 1 h, prior to the pull-down experiments with the peptide beads. Lactoferrin competition was assessed by addition of molar ratios (sLRP:lactoferrin) of 1:1, 1:10, and 1:100 prior to peptide bead pull-down experiments. Heparin competition was assessed by addition of a 1:1 or 1:2 molar ratio (sLRP:heparin) prior to pull-down experiments. Sensitivity to EDTA was assessed by performing the pull-down experiment in MB150EDTA buffer, which contained 20 mM EDTA. Following the capture of the sLRPs, the beads were washed twice with MB150 containing 0.1% Tween 20 and loaded onto a 10% reducing SDS−PAGE gel. Captured sLRPs were visualized by Western blot analysis using a polyclonal antibody raised against each sLRP.

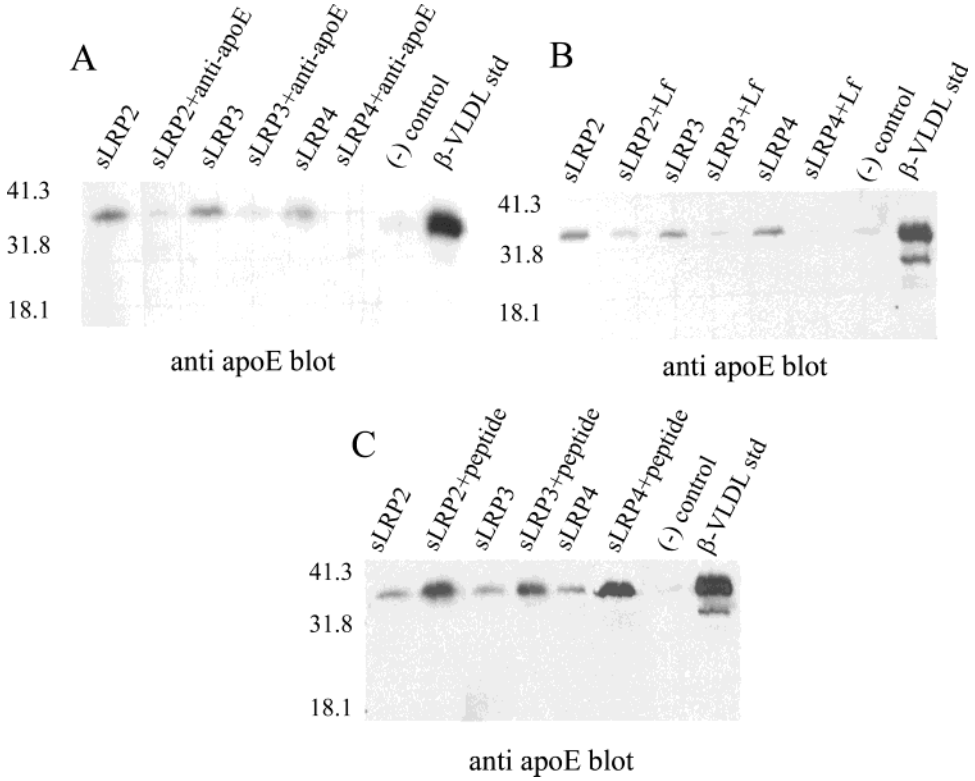

FIGURE 1: Pull-down experiment in which binding of apoE-enriched β-VLDL to each sLRP was studied. ApoE-enriched β-VLDL particles (Intracel, Inc.) (7.5 μg) were mixed with 5 μg of each sLRP−FLAG fragment (2, 3, and 4) in a volume of 1 mL at 37 °C for 2 h. ApoE−sLRP−FLAG complexes were captured using anti-FLAG M2−agarose beads and subjected to reducing 13% SDS−PAGE. Control experiments in which no sLRP−FLAG was added were used to detect nonspecific binding of apoE to the anti-FLAG−agarose beads. (A) Capture of apoE with each sLRP−FLAG in the presence and absence of a polyclonal antibody raised to apoE. (B) Capture of apoE with each sLRP−FLAG in the presence and absence of lactoferrin. (C) Capture of apoE with each sLRP−FLAG in the presence and absence of apoE(130−149).

Circular Dichroism. CD spectra were collected using an AVIV 202 instrument. CD spectra were acquired at a protein concentration of 40 μM in a cell with a path length of 0.1 cm. Samples of sLRP2 (100 μL) were prepared in MB150, and spectra were recorded at 25 °C. To one sample was added 2 μL of a 500 mM EDTA solution. The uncorrected ellipticity of each sample was plotted.

Surface Plasmon Resonance (SPR) Analysis of sLRP−ApoE Peptide Interaction. All SPR analyses were performed on a Biacore 3000 instrument. Each apoE peptide was coupled to a streptavidin (SA) sensor chip via the N-terminal biotin tag. The coupling was achieved by passing a 1 μg/mL solution of each apoE peptide in MB500 buffer over a preconditioned SA sensor chip until the desired response was achieved. Coupling to the SA sensor chip was carried out in MB500 buffer to collapse the dextran matrix, preferentially coupling the apoE peptide to surface-exposed streptavidin molecules. Binding experiments were carried out with 300 response units (RU) (300 pg/mm^2) of apoE(141−155)^2 and 50−300 response units (55−300 pg/mm^2) of apoE(130−149) coupled to the chip surface. Results of binding to a control surface to which no peptide had been coupled were subtracted from each data set. Sensorgrams were collected from a series of sLRP injections made in MB150 buffer. Injections over apoE(130−149) were at concentrations of 50, 75, 100, 200, 300, and 500 nM; injections over apoE(141−155)^2 were at concentrations of 125, 250, 500, and 1000 nM, and injections over apoE(130−149,Arg142Glu) and apoE(130−149,Lys143Glu) were at concentrations of 100, 200, 300, 400, and 500 nM. The flow rate was 5 μL/min, and the interaction of the peptide and sLRP was not limited by mass transport as determined by a flow rate dependence test (data not shown). Between each injection, the surface was regenerated with a 2 min injection of 1 M NaCl. The kinetic constants (k_a, k_d, and K_D) were extracted by globally fitting each series of injections to a 1:1 binding model with a drifting baseline using Biaevaluation version 3.1. Goodness of fit was assessed using the χ^2 value which correlates the subtracted data and the global fits generated by Biaevaluation version 3.1.

SPR Analysis of the Interaction of ApoE(130−149) and ApoE(141−155)^2 with Heparin. Binding of heparin to each apoE peptide was also assessed by SPR. Again, the peptides were immobilized at 50 RU for apoE(130−149) and 300 RU for apoE(141−155)^2. Sensorgrams were collected from a series of heparin injections made in MB150 buffer. The heparin concentrations were 1.56, 3.125, 6.25, 12.5, 25, and 50 nM for apoE(130−149) and 1, 2.5, 5, 12.5, 25, and 50 nM for apoE(141−155)^2. Between each injection, the surface was regenerated with a 2 min injection of 1 M NaCl. Data are presented as a subtraction of data collected from the control surface and data collected from each apoE peptide surface.

RESULTS

Characterization of ApoE(141−155)^2 and ApoE(130−149). The sequences and molecular weights from MALDI-

TOF mass spectrometry (with the additional N-terminal biotin tag) are given in Table 1. The peptides were shown to be soluble in aqueous buffer, and size-exclusion chromatography showed that apoE(141−155)^2 was dimeric while apoE(130−149) was monomeric (data not shown).

Solution Binding Studies of ApoE-Enriched β-VLDL Particles. Each of the sLRPs bound equivalently to apoE-enriched β-VLDL particles in solution. In these experiments, C-terminally FLAG-tagged sLRPs were incubated with apoE-enriched β-VLDL particles in solution prior to being captured by monoclonal anti-FLAG M2 antibody−agarose beads. The binding of β-VLDL particles was not inhibited by preincubation of the sLRPs with a large excess of the receptor-associated protein (RAP), nor was it affected by EDTA treatment (*23*). The binding was completely inhibited by addition of a polyclonal antibody raised against apoE (Figure 1A) and lactoferrin (Figure 1B). Interestingly, addition of apoE(130−149) caused an increase in the amount of apoE captured by each sLRP (Figure 1C). The lack of apoE(130−149) competition and potentiation of apoE binding was also reported by Nikoulin *et al.* (*25*), who observed a 7−12-fold increase in the rate of uptake of LDL in cultured human fibroblasts when apoE(141−155)^2 was added.

Solution Binding Studies of ApoE(130−149) and ApoE-(141−155)^2 with Each sLRP. The binding of the sLRPs to each peptide bound to streptavidin−agarose beads was assessed by solution binding assays. Captured sLRPs were separated by reducing 10% SDS−PAGE and probed by Western blot analysis using polyclonal antibodies raised to each individual sLRP. All three sLRPs bound to apoE(141−155)^2 (Figure 2A) and apoE(130−149) (Figure 2B), and no binding to the apoE(130−149) scrambled control peptide or to the streptavidin−agarose beads was observed (Figure 2B). Binding of all three sLRPs to apoE(141−155)^2 and apoE-(130−149) was not challenged by a 50-fold molar excess of GST−RAP (Figure 2A,B). When the pull-down experiments were performed in buffer containing 20 mM EDTA, binding was still observed (Figure 2A,B). Binding was, however, challenged by human lactoferrin (Figure 2C). Thus, the characteristics of binding of each peptide to each sLRP were similar to those previously observed with native, full-length apoE in β-VLDL particles (Figure 1 and ref *23*). This same concentration of EDTA decreased but did not completely ablate the amount of secondary structure in the sLRP2 fragment as shown by circular dichroism spectroscopy (Figure 2D). Thus, it seems that some calcium-independent structure remains that is likely to be the binding site for apoE on sLRP2. A complete study of this phenomenon is in progress.

Surface Plasmon Resonance (SPR) Binding Analysis for Binding of ApoE(130−149) and ApoE(141−155)^2 to Each sLRP. The kinetics governing the interaction between both apoE peptides and each sLRP were measured by SPR analysis. A homogeneous surface was made by coupling each N-terminally biotinylated peptide to a streptavidin (SA) sensor chip. The LC−LC linker used in biotinylating the peptides allowed for the extension of the apoE peptides from the chip surface, minimizing matrix interference (*26*). The smallest possible amount of each peptide was coupled to the surface [50−300 RU for apoE(130−149) and 300 RU for apoE(141−155)^2] so artifacts arising from overcoupling of the ligand to the sensor chip surface could be avoided (*27*).

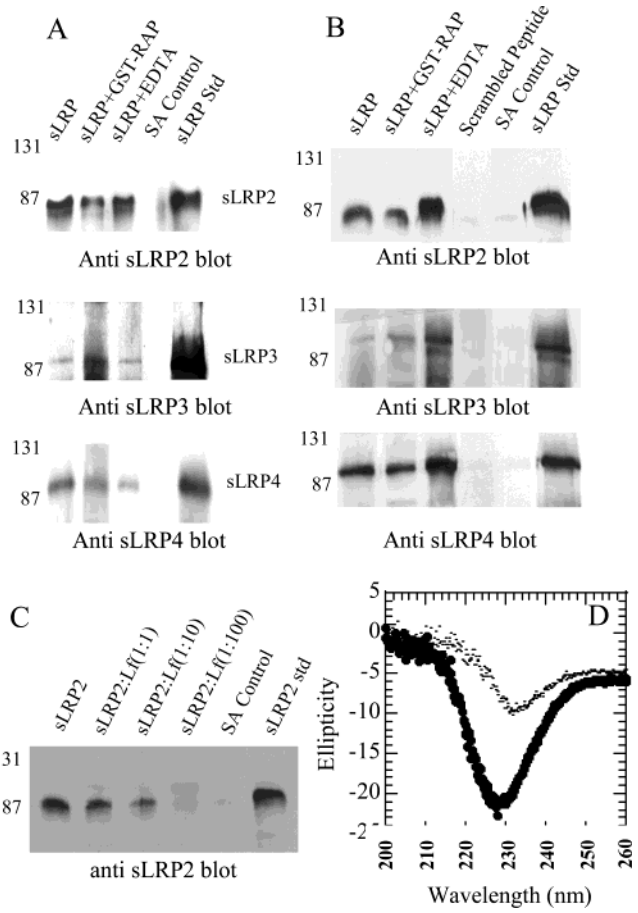

FIGURE 2: Pull-down experiment in which each sLRP was tested for binding to apoE(141−155)^2 and apoE(130−149). Each sLRP (1.7 μM) was mixed with each of the biotinylated apoE peptides bound to streptavidin−agarose beads (~10 μM) and allowed to form a complex. Captured sLRPs were electrophoresed via reducing 10% SDS−PAGE, and Western blot analysis was performed with antibodies specific to each sLRP. Control experiments were carried out in which no peptide had been bound to the streptavidin beads. The ability of either 20 mM EDTA or a 50-fold molar excess of GST−RAP to inhibit binding was also assessed. (A) Western blot of captured sLRPs with apoE(141−155)^2. (B) Western blot of captured sLRPs with apoE(130−149). (C) Capture of sLRP2 by apoE(130−149) in the presence of increasing concentrations of lactoferrin. (D) Circular dichroism spectra of sLRP2 (large symbols) and sLRP2 to which EDTA had been added (final concentration of 20 mM) (small symbols).

A representative overlay of subtracted sensorgrams of sLRP2, -3, and -4 injected over an apoE(130−149) surface showed that each of the sLRPs bound with similar kinetic parameters (Figure 3A−C). Interestingly, binding to apoE(141−155)^2 was only observed after incubation of the peptide in 500 mM NaCl (data not shown). After the solution had been pulsed with high salt, the binding kinetics were remarkably similar for the two different apoE mimetic peptides (Table 2). The binding affinity (K_D) was approximately 150 nM, which is similar to other reported binding affinities for ligands to LRP1, as measured by SPR (*28*, *29*).

Surface Plasmon Resonance Studies of ApoE(130−149, Arg142Glu) and ApoE(130−149,Lys143Glu) with sLRP2. Previous mutagenesis studies showed that mutation of Lys143 to Ala decreased the overall level of binding of full-length apoE in DMPC micelles to cell surface receptors by 90% (*16*). These experiments did not distinguish between binding to the LDL receptor and/or LRP1. Also, we obtained

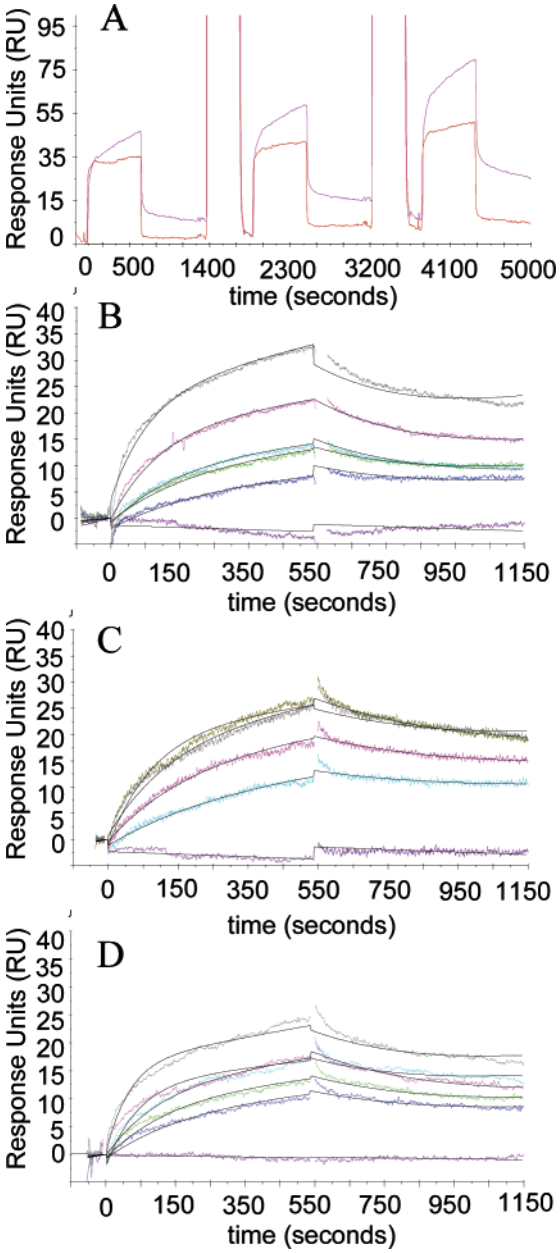

FIGURE 3: Representative sensorgrams of binding of sLRP2, -3, and -4 to apoE(130−149). ApoE(130−149) was coupled (50 RU) to a streptavidin (SA) sensor chip by way of the N-terminal biotin. Each sLRP was passed at the indicated concentrations over the surface containing apoE(130−149) and a control surface containing streptavidin at a flow rate of 5 μL/min in MB150 buffer. Panel A shows the raw, unsubtracted data (red lines for the blank SA surface and pink lines for the peptide-bound surface). For panels B−D, the sensorgrams represent the subtracted data (colored lines) and the global fits (black lines). For each experiment, the following concentrations of sLRPs were used: 50 (blue), 75 (green), 100 (cyan), 200 (magenta), 300 (gray), and 500 (brown). (B) Overlay of sLRP2 injections with global fits. (C) Overlay of sLRP3 injections with global fits. (D) Overlay of sLRP4 with global fits.

quantitative information with regard to how mutations affected the kinetics of binding to each sLRP. SPR experiments were therefore performed in which two different apoE mutant peptides (Arg142Glu and Lys143Glu) were coupled homogeneously to streptavidin chip surfaces at 300 RU via N-terminal biotin tags. Injections of varying concentrations of sLRP2 were made over each mutant peptide, and the binding kinetics were determined from the data (Figure 4A,B). Only apoE(130−149,Lys143Glu) exhibited a 10-fold decrease in binding affinity (K_D) for sLRP2 (Table 3). The 10-fold decrease in K_D is the result of a 29-fold decrease in the k_a as compared to the kinetics observed for wild-type

Table 2: Kinetic Constants for Binding of sLRP to ApoE(141−155)[2] and ApoE(130−149)

sLRP fragment	k_a (M^{-1} s^{-1})	k_d (s^{-1})	K_D (nM)	χ^2	R_{max}
		ApoE(141−155)[2]			
sLRP2	1.8×10^4	2.9×10^{-3}	160	0.358	32.5
sLRP3	1.1×10^4	2.1×10^{-3}	190	0.322	28.4
sLRP4	1.94×10^4	2.2×10^{-3}	118	0.338	21.5
		ApoE(130−149)			
sLRP2	2.1×10^4	2.7×10^{-3}	129	0.434	28.2
sLRP3	1.2×10^4	1.6×10^{-3}	124	0.497	27.0
sLRP4	4.3×10^4	2.2×10^{-3}	51	0.51	18.2

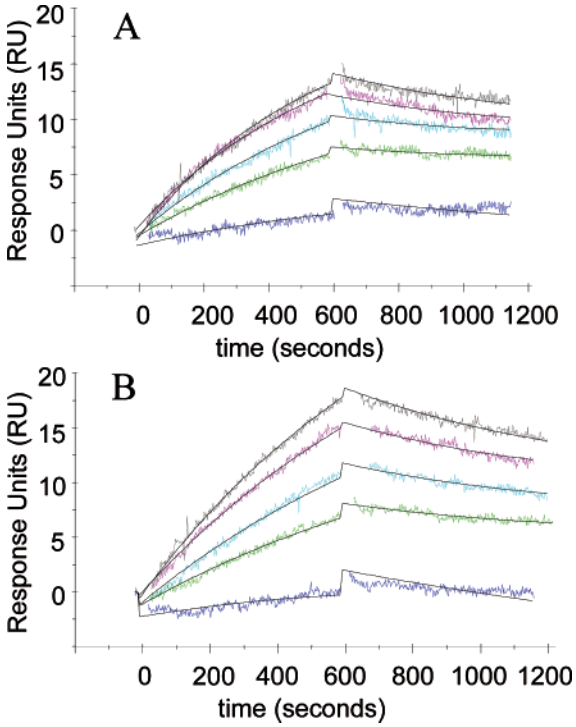

FIGURE 4: Representative sensorgrams of binding of sLRP2 to two mutant apoE(130−149) peptides. Each mutant peptide was biotinylated at the N-terminus, and 350 RU was coupled to a streptavidin (SA) sensor chip. sLRP2 was passed at increasing concentrations over an experimental surface containing each apoE peptide mutant and a control surface containing streptavidin at a flow rate of 5 mL/min in MB150 buffer. Each sensorgram shows the subtracted data (colored lines) and the global kinetic fits (black lines). For each experiment, the following concentrations of sLRP2 were used: 100 (blue), 200 (green), 300 (cyan), 400 (magenta), and 500 nM (gray). (A) Overlay of a series of sensorgrams of sLRP2 injections over apoE(130−149,Arg142Glu). (B) Overlay of a series of sensorgrams of sLRP2 injections over apoE(130−149, Lys143Glu). Because the binding was so slow and the sLRP concentrations required to observe binding were so high, it was not possible to reliably observe the saturation of the flowing association event.

Table 3: Kinetic Constants for Binding of Mutant ApoE(130−149) Peptides to sLRP2

apoE(130−149) mutant	k_a (M^{-1} s^{-1})	k_d (s^{-1})	K_D (nM)	χ^2	R_{max}
Arg142Glu	2.7×10^3	9.4×10^{-4}	348	0.158	27.1
Lys143Glu	7.2×10^2	9.4×10^{-4}	1300	0.134	109

apoE(130−149) with sLRP2. The dissociation rate also decreased 3-fold (Table 3). Mutation of Arg142 to Glu decreased both the k_a and the k_d slightly so that the overall K_D was only 2−3-fold reduced compared to that of the wild type.

Surface Plasmon Resonance of ApoE(130−149) and ApoE(141−155)^2 *Binding to Heparin and Competition of sLRP Solution Binding to Each ApoE Peptide with Heparin.* ApoE is known the bind tightly to cell surface heparan sulfate (*12*). The proposed binding site for heparin and/or heparan sulfate in apoE is located in the N-terminal domain, in the proximity of the proposed site of interaction with cell surface receptors (*12*). Although the mechanism of receptor recognition is not known, one hypothesis is that heparin and LRP1 operate in a hand-off mechanism whereby ligands first bind to cell surface heparin and then are handed off to LRP1 for internalization (*30*, *31*). SPR was again used to probe heparin binding to the bioactive apoE peptides. The equilibrium binding constant for heparin binding to each of the apoE peptides immobilized on the streptavidin chip was in the low nanomolar range. The k_a was very fast, and the k_d was near zero (Figure 5A,B). The binding of heparin to these peptides is consistent with previous reports suggesting overlap between the heparin binding site and the receptor binding site, in the region of residues 140−150 of apoE (*12*).

We also tested whether heparin could compete for binding of sLRP to apoE(130−149) in solution-based assays. For these experiments, sLRP and heparin were mixed in 1:1 and 2:1 (heparin:sLRP) molar ratios and each mixture of sLRP and heparin was pulled down with apoE(130−149)−agarose beads. Heparin was able to effectively compete for all three sLRPs binding to apoE(130−149) at a molar ratios above 1:1 (Figure 6).

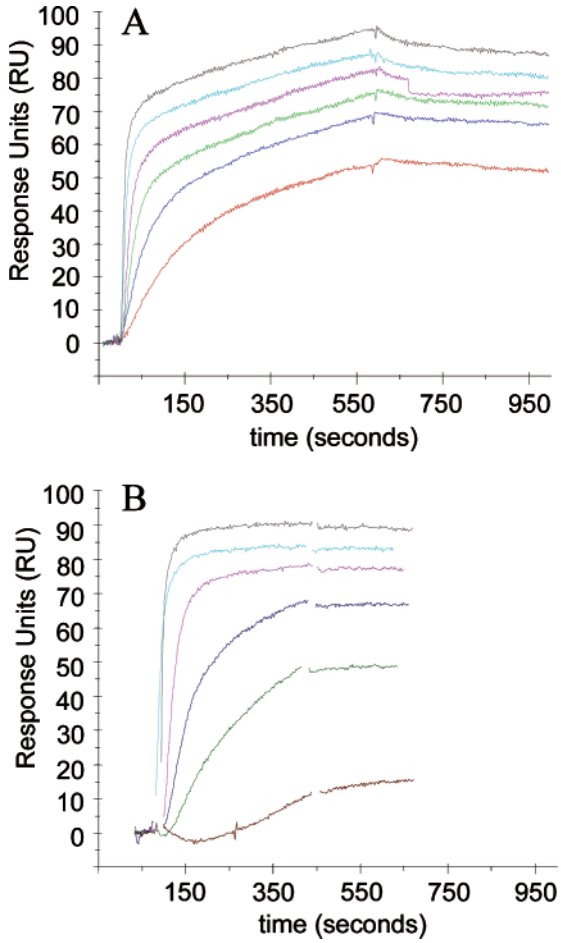

FIGURE 5: Representative sensorgrams of increasing concentrations of heparin binding to apoE(130−149) and apoE(141−155)^2. For each experiment, 300 RU of each peptide was coupled to a streptavidin chip, via the N-terminal biotin tag. As before, the subtracted sensorgrams are shown. Injections of heparin were made at 5 mL/min in MB150 buffer. (A) Sensorgram overlay of heparin at increasing concentrations [1.56 (red), 3.125 (light blue), 6.25 (light green), 12.5 (magenta), 25 (cyan), and 50 nM (gray)] binding to apoE(130−149). (B) Sensorgram overlay of heparin at increasing concentrations [1 (brown), 2.5 (dark green), 5 (dark blue), 12.5 (magenta), 25 (cyan), and 50 nM (gray)] binding to apoE(141−155)^2. Because the heparin binding is so rapid and the heparin concentrations required to observe binding were so low, it was possible to observe the saturation of the flowing association event.

DISCUSSION

We have previously shown that the three complete LDL-like homology domains in the extracellular domain of LRP1 are able to bind full-length native apoE-enriched β-VLDL particles. The binding was not affected by competition with GST−RAP or treatment with EDTA (*23*). In that work, we showed that GST−RAP does compete for binding of the receptor binding domain of α2-macroglobulin. Furthermore, addition of EDTA markedly decreased the level of binding of RAP to all three sLRPs and of the receptor binding domain of α2-macroglobulin to sLRP2 (*23*). Thus, the lack of EDTA and RAP inhibition seems not to be universal for all ligands. The lack of inhibition of apoE binding by RAP is consistent with an allosteric mechanism proposed by van Zonneveld and colleagues who found that RAP was not very effective in inhibiting the binding of ligands to sLRP2, but very effective in inhibiting binding to the full-length molecule (*29*). Binding was specific, however, as it could be challenged by an anti-ApoE polyclonal antibody and by lactoferrin, consistent with other reports (*23*, *32*). In the work presented here, we build upon these previous results to narrow the LRP1 binding site on apoE by using bioactive apoE peptides (*33*). Peptides derived from the N-terminal domain of apoE have been implicated in a number of different cellular response events such as cytotoxicity, cytostatic effects, microglial activation, and G-protein-coupled receptor-promoted Ca^{2+} influx (*18*−*21*). These peptides include the proposed binding epitope for the LDL receptor; however, no direct evidence of whether the peptides indeed interact with LRP1 has been obtained. Thus, the question of whether these peptides elicit cellular responses via LRP1 remains. Two of the most commonly used bioactive apoE peptides were first used in qualitative binding assays. Each peptide was able to bind to each sLRP fragment. The binding characteristics were identical to those of full-length apoE. Binding was unaffected by inhibition with GST−RAP or EDTA, but was challenged by lactoferrin. These observations recapitulate the binding properties of the sLRPs with full-length apoE in β-VLDL particles (*23*) and suggest that the bioactive apoE peptides bind to the same site as full-length apoE on LRP1.

For both peptides, the association rate was found to be on the order of 10^4 M^{-1} s^{-1}, which is the same order of magnitude for a large number of protein−protein interactions (*27*, *34*). For both peptides, dissociation rates were found to

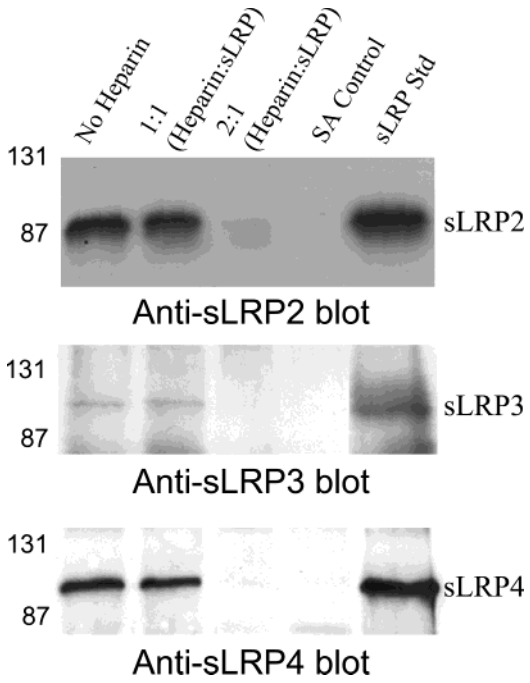

FIGURE 6: Solution binding experiment in which each sLRP was tested for binding to apoE(130−149) in the presence and absence of an increasing number of molar equivalents of heparin. Each sLRP was mixed with apoE(130−149) bound to streptavidin−agarose beads and allowed to form a complex. Heparin was added at the indicated concentrations and was mixed simultaneously with each sLRP and peptide−agarose beads. Molar equivalents of heparin were based on the average molecular weight of heparin being 20 000. Control experiments in which no peptide had been bound to the streptavidin beads were carried out. Captured sLRPs were run on reducing 10% SDS−PAGE, and Western blot analysis was performed with antibodies specific to each sLRP.

be on the order of 10^{-3} s^{-1}, and this slow k_d directly accounts for the relatively tight K_D. The two peptides bound to each sLRP with similar kinetics and affinities in the 100 nM range. This remarkably tight binding for such a small peptide is consistent with previous reports in which binding to cell surfaces was assessed. An approximate equilibrium constant of 50 nM was reported for apoE(130−149) binding to cell surface receptors on macrophages, fit to a 1:1 binding model (*19*). The cell surface undoubtedly contains several different receptors, as well as heparin sulfate proteoglycans that most likely contributed to the measured binding affinities. Cytotoxicity studies by Tolar *et al.* (*22*) have reported a half-maximal effective concentration for causing neuronal cell death of 1 μM for apoE(141−155)^2. Our results show that full binding competency is not achieved prior to incubation of apoE(141−155)^2 with a high-salt buffer, so it may be that only part of the peptide used in the cytotoxicity studies was binding competent.

Importantly, our results demonstrate that the bioactive apoE peptides bind tightly to LRP1 in a purified system. Several studies showing cellular responses upon treatment with the bioactive apoE peptides could not definitively implicate LRP1 because most cells express several apoE-binding receptors. Furthermore, in some studies, RAP competition partially ablated the bioactivity of the peptides (*19*, *22*), while in other studies, addition of RAP did not have any effect (*18*, *20*). Our results show that RAP does not directly inhibit binding of the peptides to LRP1. Given that LRP1 is a *bona fide* signaling receptor and that the peptides bind with slow dissociation rates, it is very likely that the cellular responses are due to direct binding of the peptides to LRP1 (*35*−*37*).

Lysine 143 had previously been shown to be important for binding of apoE to cell surface receptors (*16*). This mutation was incorporated into the apoE(130−149) peptide, and the overall K_D for binding to sLRP2 decreased by 10-fold. This result is consistent with the idea that Lys143 is important for creating an electrostatic attraction between apoE and LRP1, an effect that is reflected primarily in the association rate. This suggests that the association may be electrostatically driven, while the slow dissociation rate may be due to interaction with hydrophobic residues within the short sequence of residues 141−155 of apoE. Further experiments are planned to test both of these hypotheses. Arginine 142 was also mutated, but it was observed to have a much smaller effect on the overall K_D, although again the primary defect was an observed decrease in the association rate. Interestingly, a naturally occurring Arg142Cys mutation in apoE2 has been shown to decrease the level of binding to the LDL receptor to some 20% of that of the wild type and has been identified as the causative mutation in this form of type III hyperlipoproteinemia (*38*).

Heparin bound to each of the apoE peptides, which was expected given that they contain previously identified heparin binding residues (*12*). The SPR experiments showed that heparin binding was essentially irreversible with k_d values too slow to measure. This may be due to the interaction of one heparin with multiple peptides on the SPR chip, and the SPR results should be mainly interpreted in a qualitative manner also because of the heterogeneous nature of the heparin that was the flowing analyte. In solution binding experiments, binding of each sLRP to apoE(130−149) was effectively challenged by heparin at molar ratios above 1:1. These results are consistent with previous studies in which the cellular responses caused by these two peptides were alleviated by the addition of heparin (*21*, *39*). The solution binding studies argue against the proposed "hand-off" mechanism in which apoE would first bind weakly to cell surface heparan sulfates and then be handed off to LRP1. Instead, a more likely mechanism is one in which the β-VLDL particles contain several molecules of apoE, some that bind to the cell surface heparan sulfates and others that bind to LRP1. The heparan sulfate binding most likely retains the β-VLDL particles at the cell surface until binding to LRP1 can occur. The entire complex is then most likely recruited for internalization.

All of the results presented here suggest that these bioactive apoE peptides may, in fact, be acting in a manner very similar to that of full-length apoE. Because apoE must be incorporated into lipids to bind to LDL receptor family members, it has been difficult to obtain quantitative binding kinetics for binding of the full-length protein to receptors. These peptides provide an attractive alternative because they are soluble, they do not require lipid for binding, and they appear to recapitulate the binding characteristics of the full-length protein.

REFERENCES

1. Mahley, R. W., and Innerarity, T. L. (1983) Lipoprotein receptors and cholesterol homeostasis, *Biochim. Biophys. Acta 737*, 197−222.

2. Boyles, J. K., Notterpek, L. M., and Anderson, L. J. (1990) Accumulation of apolipoproteins in the regenerating and remyelinating mammalian peripheral nerve, *J. Biol. Chem. 265*, 17805−17815.
3. Skene, J. H. P., and Shooter, E. M. (1983) Denervated sheath cells secrete a new protein after injury, *Proc. Natl. Acad. Sci. U.S.A. 80*, 4169−4173.
4. Corder, E. H., Saunders, A. M., Strittmatter, W. J., Schmechel, D., Gaskell, P. C., Small, G. W., Roses, A. D., Haines, J. L., and Pericak-Vance, M. (1993) Gene does of apolipoprotein E type 4 allele and the risk of Alzheimer's disease in late onset families, *Science 261*, 921−923.
5. Diedrich, J. F., Minnigan, H., Carp, R. I., Whitaker, J. N., Race, R., Frey, W. H., and Haase, A. T. (1991) Neuropathological changes in scrapie and Alzheimer's disease are associated with increased expression of apolipoprotein E and cathepsin D in astrocytes, *J. Virol. 65*, 4759−4768.
6. Strittmatter, W. J., Saunders, A. M., Schmechel, D., Pericak-Vance, M., Enghild, G., Salvesen, S., and Roses, A. D. (1993) Apolipoprotein E: high-avidity binding to β-amyloid and increased frequency of type 4 allele in late-onset familial Alzheimer's disease, *Proc. Natl. Acad. Sci. U.S.A. 90*, 1977−1981.
7. Rall, S. C. J., Weisgraber, K. H., and Mahley, R. W. (1982) Human Apolipoprotein E. The Complete Amino Acid Sequence, *J. Biol. Chem. 257*, 4171−4178.
8. Weisgraber, K. H. (1994) Apolipoprotein E: Structure−Function Relationships, *Adv. Protein Chem. 45*, 249−302.
9. Wilson, C., Wardell, M. R., Weisgraber, K. H., Mahley, R. W., and Agard, D. A. (1991) Three-dimensional structure of the LDL receptor-binding domain of human apolipoprotein E, *Science 252*, 1817−1822.
10. Weisgraber, K. L., Innerarity, T. L., Harder, K. J., Mahley, R. W., Milne, R. W., Marcel, Y. L., and Sparrow, J. T. (1983) The Receptor Binding Domain of Human Apolipoprotein E, *J. Biol. Chem. 258*, 12348−12354.
11. Innerarity, T. L., Friedlander, E. J., Rall, S. C., Jr., Weisgraber, K. H., and Mahley, R. W. (1983) The Receptor-binding Domain of Human Apolipoprotein E, *J. Biol. Chem. 258*, 12341−12347.
12. Weisgraber, K. H., Rall, S. C. J., Mahley, R. W., Miline, R. W., Marcel, Y. L., and Sparrow, J. T. (1986) Human apolipoprotein E. Determination of the heparin binding sites of apolipoprotein E3, *J. Biol. Chem. 261*, 2068−2076.
13. Saito, H., Dhanasekaran, P., Nguyen, D., Baldwin, F., Weisgraber, K. H., Wehrli, S., Phillips, M. C., and Lund-Katz, S. (2003) Characterization of the Heparin Binding Sites in Human Apolipoprotein E, *J. Biol. Chem. 278*, 14782−14787.
14. Zannis, V. I., and Breslow, J. L. (1981) Human very low-density lipoprotein apolipoprotein E isoprotein polymorphism is explained by genetic variation and posttranslational modification, *Biochemistry 20*, 1033−1041.
15. Brenninkmeijer, B. J., Stuyt, P. M. J., Demacker, P. N. M., Stalenhoef, A. F. H., and van't Laar, A. (1987) Catabolism of chylomicron remnants in normolipidemic subjects in relation to the apoprotein E phenotype, *J. Lipid Res. 28*, 361−370.
16. Lalazar, A., Weisgraber, K. H., Rall, S. C. J., Gilad, H., Innerarity, T. L., Levanon, A. Z., Boyles, J. K., Amit, B., Gorecki, M., Mahley, R. W., and Vogel, T. (1988) Site-specific Mutagenesis of human apolipoprotein E. Receptor binding activity of variants with single amino acids substitutions, *J. Biol. Chem. 263*, 3542−3545.
17. Marques, M. A., Tolar, M., Harmony, J. A. K., and Crutcher, K. A. (1996) A thrombin cleavage fragment of apolipoprotein E exhibits isoform specific neurotoxicity, *NeuroReport 7*, 2529−2532.
18. Moulder, K. L., Narita, M., Chang, L. K., Bu, G., and Johnson, E. M., Jr. (1999) Analysis of a novel mechanism of neuronal toxicity produced by an apolipoprotein E derived peptide, *J. Neurochem. 72*, 1069−1080.
19. Misra, U. K., Adlakha, C. L., Gawdi, G., McMillian, M. K., Pizzo, S. V., and Laskowitz, D. T. (2001) Apolipoprotein E and Mimetic Peptides Initial A Calcium Dependent Signaling Response In Macrophages, *J. Leukocyte Biol. 70*, 677−683.
20. Laskowitz, D. T., Thekdi, A. D., Thekdi, S. D., Han, S. K. D., Myers, J. K., Pizzo, S. V., and Bennett, E. R. (2001) Downregulation of microglial activation by apolipoprotein E and apoE-mimetic peptides, *Exp. Neurol. 167*, 74−85.
21. Clay, M. A., Anantharamaiah, G. M., Mistry, M. J., Balasubramaniam, A., and Harmony, J. A. K. (1995) Localization of a Domain in Apolipoprotein E with both Cytostatic and Cytotoxic Activity, *Biochemistry 34*, 11142−11151.
22. Tolar, M., Marques, M. A., Harmony, J. A. K., and Crutcher, K. A. (1997) Neurotoxicity of the 22-kDa thrombin-cleavage fragment of apolipoprotein E and related synthetic peptides is receptor-mediated, *J. Neurosci. 17*, 5678−5686.
23. Croy, J. E., Shin, W. D., Knauer, M. F., Knauer, D. J., and Komives, E. A. (2003) All three LDL receptor homology region of the LDL receptor-related protein bind multiple ligands, *Biochemistry 42*, 13049−13057.
24. Orlando, R. A., and Farquhar, M. G. (1994) Functional domains of the receptor-associated protein (RAP), *Proc. Natl. Acad. Sci. U.S.A. 91*, 3161−3165.
25. Nikoulin, I. R., and Curtiss, L. K. (1998) An apolipoprotein E synthetic peptide targets to lipoproteins in plasma and mediates both cellular lipoprotein interactions in vitro and acute clearance of cholesterol-rich lipoproteins in vivo, *J. Clin. Invest. 101*, 223−234.
26. Baerga-Ortiz, A., Rezaie, A. R., and Komives, E. A. (2000) Electrostatic Dependence of the Thrombin-Thrombomodulin Interaction, *J. Mol. Biol. 296*, 651−658.
27. Myszka, D. G. (1997) Kinetic analysis of macromolecular interactions using surface plasmon resonance biosensors, *Curr. Opin. Biotechnol. 8*, 50−57.
28. Neels, J. G., van den Berg, B. M. M., Lookene, A., Olivecrona, G., Pannekoek, H., and van Zonneveld, A. J. (1999) The second and fourth cluster of class A cysteine-rich repeats of the low-density lipoprotein receptor-related protein share ligand binding properties, *J. Biol. Chem. 274*, 31305−31311.
29. Horn, I. R., van den Berg, B. M. M., van der Meijden, P. Z., Pannekoek, H., and van Zonneveld, A. J. (1997) Molecular analysis of ligand binding to the second cluster of complement-type repeats of the low-density lipoprotein receptor-related protein, *J. Biol. Chem. 272*, 13608−13613.
30. Ji, Z.-S., Fazio, S., Lee, Y.-L., and Mahley, R. W. (1994) Secretion-capture role for apolipoprotein E in remnant lipoprotein metabolism involving cell surface heparan sulfate proteoglycans, *J. Biol. Chem. 269*, 2764−2772.
31. Mentz, S., de Lacalle, S., Baerga-Ortiz, A., Knauer, M. F., Knauer, D. J., and Komives, E. A. (1999) Mechanism of thrombin clearance by human astrocytoma cells, *J. Neurochem. 72*, 980−987.
32. Willnow, T. E., Goldstein, J. L., Orth, K., Brown, M. S., and Herz, J. (1992) Low-density lipoprotein receptor-related protein and GP330 bind similar ligands including plasminogen activator-inhibitor complexes, and lactoferrin, an inhibitor of chylomicron remnant clearance, *J. Biol. Chem. 267*, 26172−26180.
33. Dyer, C. A., Smith, R. S., and Curtiss, L. K. (1991) Only multimers of a synthetic peptide of human apolipoprotein E are biologically active, *J. Biol. Chem. 266*, 15009−15015.
34. Koren, R., and Hammes, G. G. (1976) A kinetic study of protein−protein interactions, *Biochemistry 15*, 1165−1171.
35. Misra, U. K., Chu, T. C. C., Gawdi, G., and Pizzo, S. V. (1994) The relationship between low density lipoprotein/α2-macroglobulin receptors and the newly described α2M signaling receptor, *J. Biol. Chem. 269*, 18803−18806.
36. van der Geer, P. (2002) Phosphorylation of LRP1: regulation of transport and signal transduction, *Trends Cardiovasc. Med. 12*, 160−165.
37. Pietrzik, C. U., Busse, T., Merriam, D. E., Weggen, S., and Koo, E. H. (2002) The cytoplasmic domain of the LDL receptor-related protein regulates multiple steps in APP processing, *EMBO J. 21*, 5691−5700.
38. Horie, Y., Fazio, S., Westerland, J. R., Weisgraber, K. H., and Rall, S. C. J. (1992) The functional characteristics of a human apolipoprotein E vairant (cysteine at residue 142) may explain its association with dominant expression of type III hyperlipoproteinemia, *J. Biol. Chem. 267*, 1962−1968.
39. Bazin, H. G., Marques, M. A., Owens, A. P. I., Linhardt, R. J., and Crutcher, K. A. (2002) Inhibition of apolipoprotein E-related neurotoxicity by glycosaminoglycans and their oligosaccharides, *Biochemistry 41*, 8203−8211.

BI036208P